Published in final edited form as:
Gene Expr Patterns. 2008 September ; 8(7-8): 486–493. doi:10.1016/j.gep.2008.06.006.

uPARAP Expression during Murine Lung Development

Leah Smith[1], **Teresa E Wagner**[1], **Isham Huizar**, and **Lynn M Schnapp**[2]
Division of Pulmonary and Critical Care Medicine, Department of Medicine, Harborview Medical Center, University of Washington, Seattle, WA 98104

Abstract

Lung remodeling requires active collagen deposition and degradation. Urokinase plasminogen activator receptor-associated protein (uPARAP), or Endo 180, is a cell surface receptor for collagens, which leads to collagen internalization and degradation. Thus, uPARAP-mediated collagen degradation is an additional pathway for matrix remodeling in addition to matrix remodeling mediated by matrix metalloproteinases and cathepsins. Using immunohistochemistry, we demonstrate extensive uPARAP expression in the mesenchyme throughout murine lung development. By immunofluorescence, we demonstrate significant overlap of uPARAP expression with collagen IV expression, but minimal overlap with collagen I expression in the developing murine lung. Finally, we compared lung development between wild-type and uPARAP −/− mice, and found no significant histologic differences, indicating the presence of alternative collagen degradation pathways during murine lung development.

Keywords

lung development; collagen; uPARAP; Endo 180

1. Results and Discussion

Urokinase plasminogen activator receptor-associated protein (uPARAP), or Endo180, is a newly described cell-surface receptor that binds and internalizes collagens, including types I, IV, and V, targeting them for lysosomal degradation (Behrendt et al. 2000; Engelholm et al. 2003; Engelholm et al. 2001; Kjoller et al. 2004). A member of the mannose receptor family, uPARAP is expressed on macrophages and mesenchymal cells, including chondrocytes and some fibroblasts (Howard et al. 2004; Sheikh et al. 2000). Mesenchymal cells that lack uPARAP are unable to internalize collagen (Curino et al. 2005; East et al. 2003; Engelholm et al. 2003; Kjoller et al. 2004; Madsen et al. 2007; Mousavi et al. 2005). In addition to its role in collagen internalization and degradation, uPARAP contributes to the adhesion and migration of collagen in vitro (Engelholm et al. 2003). uPARAP may also play a role in human gingival re-epithelialization and remodeling after injury (Honardoust et al. 2006). In addition, uPARAP is expressed in tumor stromal cells and has a role in tumor progression (Curino et al. 2005; Sulek et al. 2007).

2Address correspondence to Lynn M. Schnapp, lschnapp@u.washington.edu, Box 359640, 325 9th Ave, Seattle WA 98104, Tel 206 341-5389, Fax 206 341-5392.
[1]These authors contributed equally to the manuscript

During lung development, the matrix undergoes active remodeling during the formation and differentiation of airways, vasculature, and mature alveoli. In particular, during the saccular stage (E17.5 to post-natal day 5 (PN5)) and alveolar stage (PN5–PN30), the lung interstitium undergoes extensive remodeling with a decrease in the interstitial space, maturation and narrowing of the blood-air barrier and thinning of the newly formed alveolar septa. Such remodeling requires active collagen synthesis and degradation. Much focus has been paid to extracellular pathways of collagen degradation, including matrix metalloproteinases (MMPs) and cathepsins. Despite the known role of MMPs in matrix remodeling, knockouts of MMPs to date (MMP-2, -3, -7, -8, -9, -11, -12, -28) show no lung abnormalities and no or minor developmental phenotypes (reviewed in (Parks and Shapiro 2001) and (Greenlee et al. 2007)). The one notable exception is MMP-14 (MT1-MMP), in which the knockout mice have severe skeletal abnormalities due to impaired collagen turnover (Holmbeck et al. 1999). The mice also have abnormalities in alveolarization, demonstrating a role for collagen degradation in alveolar formation (Atkinson et al. 2005). In contrast to these other pathways of degradation, uPARAP-mediated collagen internalization and degradation allows cells to recycle collagen components, a key feature of cell housekeeping. This makes uPARAP an attractive candidate for collagen turnover during normal development. While high levels of uPARAP mRNA have been found in fetal and adult total lung tissue (Wu et al. 1996), the expression pattern has not been examined in the developing murine lung. uPARAP is known to interact with collagens, including collagens I and IV, but the spatio-temporal relationship of uPARAP to these proteins has yet to be elucidated. We determined the spatio-temporal expression of uPARAP during murine lung development by immunohistochemistry and real-time PCR. We also examined lung development in uPARAP −/− mice to further investigate the role of uPARAP in the developing lung. Finally, we analyzed uPARAP −/− mice for differences in matrix synthesis and MMP expression during lung development.

uPARAP immunoreactivity was present at the earliest time point tested, (E12.5), the early pseudoglandular stage (E12.5-16.5), when branching morphogenesis occurs (Figure 1A). uPARAP was detected on the majority of mesenchymal cells, but absent on airway epithelium. At mid-pseudoglandular stage (Fig 1, C–F), there was persistent mesenchymal immunoreactivity, however, the staining appeared more discontinuous along the mesenchymal cell surface, with more prominent staining at areas of cell-matrix interactions and less staining at cell-cell junctions. By E16.5 (Fig 1, I–J), uPARAP immunoreactivity was present in the layer beneath airway epithelium and became more pronounced during post-natal lung development (Figure 2, C–H)). No uPARAP immunoreactivity was observed on epithelial cells at any stage of development. As controls, no uPARAP immunoreactivity was observed in lungs from uPARAP −/− mice or using isotype control antibody (Figure 3 and not shown).

We also analyzed uPARAP mRNA expression during lung development by real time PCR. We found relatively consistent levels of uPARAP mRNA from E15.5 through PN2.0. At PN10, there was a significant increase in uPARAP expression compared to E15.5 (Figure 4), which decreased at later timepoints.

Since uPARAP binds and internalizes collagens, we examined the distribution of uPARAP and collagens during lung development. We first examined collagen I, a major component of interstitial matrix. Several studies have demonstrated that uPARAP is able to internalize and degrade, adhere, and migrate on collagen I (Behrendt 2004). Surprisingly, there were minimal areas of overlap of immunofluorescent staining for uPARAP and collagen I. This was particularly true in early stages of lung development. In the pseudoglandular stage (E12.5–16.5, Fig 5, A–B), collagen I immunoreactivity was prominent around developing airways without uPARAP expression. During the cannalicular stage (E 16.5–17.5, Fig 5, C–D), occasional mesenchymal immunoreactivity was detected, with continued clustering of collagen I around developing airways and vasculature, with minimal uPARAP expression. In the

saccular (E17.5-PN4) and alveolar (PN4-30) stages (Fig 5, E–H), collagen I localized along the septal tips, again without overlap with uPARAP expression.

In contrast, there was extensive overlap of uPARAP and collagen IV expression (Figure 6) in the mesenchyme at all stages of development. Highest expression of collagen IV was noted surrounding mesenchymal cells, where it overlapped with uPARAP expression. uPARAP expression, however, extended beyond areas of collagen IV expression.

We also considered whether absence of uPARAP delayed or altered lung development. We were particularly interested in the later stages of development (saccular and alveolar stages), since that is when extensive interstitial remodeling occurs with decrease in interstitium, thinning of the air-blood barrier, and formation of the mature alveolar septum. In addition, uPARAP expression was highest during the alveolar stage (Figure 4). Surprisingly, despite the extensive immunoreactivity of uPARAP during all stages of lung development in wild-type mice, there was no detectable difference between lung development in uPARAP knockout and wild-type mice (Fig 6). The onset of alveolar septal formation and degree of maturation of the alveolar septum was not appreciably different in wild-type vs. uPARAP knockout mice. There was no difference in the mean linear intercept. Lungs from adult wild type and uPARAP −/− were histologically indistinguishable. Furthermore, we examined collagen IV expression by immunofluorescence in uPARAP −/− mice throughout development and did not detect any obvious changes in expression patterns compared to wt mice (Fig 6).

There are several potential explanations for lack of lung phenotype in uPARAP −/− mice. It is possible that decreased synthesis of collagens compensates for the absence of uPARAP. To analyze this possibility, we compared collagen I and collagen IV mRNA expression in wild type and uPARAP −/− mice during lung development. We did not see any significant differences in mRNA expression between wild type and uPARAP −/− mice at any of the time points examined (Figure 8).

We also examined MMP mRNA expression to determine if there were any compensatory increases in the uPARAP −/− mice. We analyzed MMp-2, -3, -7, -9, 10, -11, -14, and -28 expression throughout lung development. We did not see any difference in expression in any of the examined MMPs, including MMP-14 (Figure 9). MMP-10 expression was not detected at any timepoint (not shown). MMP-11 (stromelysin-3) demonstrated a trend to increased expression in uPARAP −/− at PN2 and PN10, but this did not achieve statistical significance. MMP-11 is expressed in fibroblasts and was originally identified as a stromal-derived factor upregulated in breast cancer (Basset et al. 1990). However, MMP-11 is not able to degrade any of the major extracellular matrix components, including collagens, and its biological substrate and function are unknown (Matziari et al. 2007). Thus, it is an intriguing finding, but of unclear significance at this point. Since MMP activity is regulated by Tissue Inhibitors of Metalloproteinases (TIMPs), we also examined TIMP expression. Again, we did not detect any significant difference between wildtype and uPARAP −/− mice in TIMP-1, -2, or -3 expression at any timepoint (Figure 9). Finally, we did not see any difference in TGFβ expression, a major regulator of matrix remodeling (Figure 9).

We show the first detailed analysis of uPARAP expression during lung development. We found extensive expression of uPARAP within the lung mesenchyme. uPARAP co-localized extensively with collagen IV during lung development. In contrast, there was minimal overlap of uPARAP and collagen I expression during lung development. Analysis of uPARAP knockout mice shows that despite the extensive uPARAP expression during normal lung development, absence of uPARAP does not result in an overt lung phenotype or compensatory changes in expression of collagens, MMPs or TIMPS. We speculate that uPARAP may have

evolved to respond to postnatal injury and repair, in an analogous function to many of the MMPs.

2. Experimental Procedures

2.1 Tissue Specimens

This study was approved by the University of Washington Institutional Animal Care and Use Committee. uPARAP knockout mice on a FVB background were a generous gift from Thomas Bugge, MD (NIH, Bethesda, MD) (Engelholm et al. 2003). Mice (C57BL/6, FVB wt or uPARAP −/−) were time-mated and checked every morning for a vaginal plug to determine day 0.5 of gestation. Embryos were collected at different stages and lungs were dissected and immersed at 4C in serial concentrations of sucrose in PBS. Postnatal lungs were dissected and inflated with OCT and PBS at a ratio of 30:70. After sucrose preservation or OCT:PBS inflation, tissues were embedded in OCT (Tissue-Tek; Sakura Finetek, Torrance, CA) and frozen in chilled methylbutane. In addition, some postnatal lungs were fixed in 4% paraformaldehyde at 20cm of pressure then paraffin embedded.

2.2 Immunochemistry

Immunohistochemistry was performed using mouse on mouse (MOM) detection system (Vector Labs, Burlingame, CA) according to manufacturer's protocol using uPARAP mouse monoclonal antibody (2.H.9:F12) (generous gift from Lars Engelhom, PhD, Finsen Laboratory, Copenhagen, Denmark (Sulek et al. 2007)) (0.25 μg/ml) or isotype control mouse IgG1κ (eBiosciences, San Diego, CA) for 1 hour at RT. Secondary biotinylated antibody (Vector MOM Kit) was applied to samples and immunoperoxidase complexes were formed using Vectastain Elite ABC Kit (Vector). Color development was performed with DAB (Sigma Chemical; St. Louis, MO) followed by DAB enhancer (Zymed). Sections were counterstained with hematoxylin (Vector), serially dehydrated, and mounted with Permount (Sigma). Additional control sections were obtained by performing immunostaining of lung sections from uPARAP −/− mice with the uPARAP antibody. Hematoxylin and eosin (H&E) staining was performed on paraffin embedded sections. Photographs were taken through a Nikon eclipse 80i microscope using x40 and x100 lenses with a DS Camera Head DS-5M.

2.3 Immunofluorescence

Double immunofluorescence was performed with uPARAP or isotype control antibody at 2.5 μg/ml for 30 min RT, followed by M.O.M. secondary antibody (1:250), then streptavidin-conjugated Alexa 488 (Molecular Probes; Invitrogen, Eugene, OR). Sections were incubated with either polyclonal collagen I antibody (gift from Christine Abrass, MD, University of Washington, Seattle, WA) followed by Alexa 568 conjugated donkey-anti-goat antibody (Molecular Probes) or rabbit anti-mouse collagen IV antibody (Chemicon) followed by biotinylated anti-rabbit antibody (Vector) and streptavidin-conjugated Alexa 568 (Molecular Probes). Nuclei were counterstained with To-Pro-3 (Molecular Probes). Slides were mounted with Vectashield Hardset Medium (Vector). Photographs were obtained using a Nikon Eclipse TE200 inverted fluorescent microscope (Melville, NY) using 20x, 40x, and 100x oil-immersion lenses with a confocal BioRad Confocal Laser Scanning System Radiance 2000 (BioRad Laboratories, Hercules, CA) equipped with krypton-argon and red diode lasers, using LaserSharp 2000 software (BioRad). Images were superimposed and processed with Adobe Photoshop (version 7.0; San Jose, CA).

2.4 Real-time PCR

Total RNA was isolated from lungs at E15.5, E17.5, PN 2, PN 10 from wildtype FVB and uPARAP −/− mice using Qiagen RNeasy Midi Kit per manufacturer's specifications. Total

RNA was reverse-transcribed to cDNA using Applied Biosystems High-Capacity cDNA Archive Kit. Real-time PCR was done using ABI 7900HT with the use of pre-designed primers and probes (ABI TaqMan Gene Expression Assays) for HPRT (as endogenous control) and indicated genes (as target probe). Target genes included MMP-2, 3, -7, -9, -11, -14, -28, TIMP-1, TIMP-2, TIMP-3, collagen α1, collagen IV, TGFβ, uPARAP. Analysis was done using MS Excel calculating RQ by 2-DDCT. Means of more than two groups of data were compared using one-way analysis of variance (ANOVA) with Tukey's honestly significant difference (HSD) post hoc test. Statistical significance was set as $p<0.05$. As a control, real-time PCR for uPARAP was performed on lungs from uPARAP −/− mice. No signal was detected at any timepoint (not shown).

Acknowledgements

Authors thank Dr. Thomas Bugge (NIH) for providing mice and guidance and Dr. Lars Engleheim (Finsen Laboratory, Copenhagen, Denmark) for providing uPARAP antibodies and providing technical advice. This work was funded by ALA Fellowship and T32 HL07287-27 (TW) and AHA Grant-in-Aid (LMS).

References

Atkinson JJ, Holmbeck K, Yamada S, Birkedal-Hansen H, Parks WC, Senior RM. Membrane-type 1 matrix metalloproteinase is required for normal alveolar development. Dev Dyn 2005;232:1079–1090. [PubMed: 15739229]

Basset P, Bellocq JP, Wolf C, Stoll I, Hutin P, Limacher JM, Podhajcer OL, Chenard MP, Rio MC, Chambon P. A novel metalloproteinase gene specifically expressed in stromal cells of breast carcinomas. Nature 1990;348:699–704. [PubMed: 1701851]

Behrendt N. The urokinase receptor (uPAR) and the uPAR-associated protein (uPARAP/Endo180): membrane proteins engaged in matrix turnover during tissue remodeling. Biol Chem 2004;385:103–136. [PubMed: 15101555]

Behrendt N, Jensen ON, Engelholm LH, Mortz E, Mann M, Dano K. A urokinase receptor-associated protein with specific collagen binding properties. J Biol Chem 2000;275:1993–2002. [PubMed: 10636902]

Curino AC, Engelholm LH, Yamada SS, Holmbeck K, Lund LR, Molinolo AA, Behrendt N, Nielsen BS, Bugge TH. Intracellular collagen degradation mediated by uPARAP/Endo180 is a major pathway of extracellular matrix turnover during malignancy. J Cell Biol 2005;169:977–985. [PubMed: 15967816]

East L, McCarthy A, Wienke D, Sturge J, Ashworth A, Isacke CM. A targeted deletion in the endocytic receptor gene Endo180 results in a defect in collagen uptake. EMBO Rep 2003;4:710–716. [PubMed: 12835757]

Engelholm LH, List K, Netzel-Arnett S, Cukierman E, Mitola DJ, Aaronson H, Kjoller L, Larsen JK, Yamada KM, Strickland DK, Holmbeck K, Dano K, Birkedal-Hansen H, Behrendt N, Bugge TH. uPARAP/Endo180 is essential for cellular uptake of collagen and promotes fibroblast collagen adhesion. J Cell Biol 2003;160:1009–1015. [PubMed: 12668656]

Engelholm LH, Nielsen BS, Dano K, Behrendt N. The urokinase receptor associated protein (uPARAP/endo180): a novel internalization receptor connected to the plasminogen activation system. Trends Cardiovasc Med 2001;11:7–13. [PubMed: 11413046]

Greenlee KJ, Werb Z, Kheradmand F. Matrix metalloproteinases in lung: multiple, multifarious, and multifaceted. Physiol Rev 2007;87:69–98. [PubMed: 17237343]

Holmbeck K, Bianco P, Caterina J, Yamada S, Kromer M, Kuznetsov SA, Mankani M, Robey PG, Poole AR, Pidoux I, Ward JM, Birkedal-Hansen H. MT1-MMP-deficient mice develop dwarfism, osteopenia, arthritis, and connective tissue disease due to inadequate collagen turnover. Cell 1999;99:81–92. [PubMed: 10520996]

Honardoust HA, Jiang G, Koivisto L, Wienke D, Isacke CM, Larjava H, Hakkinen L. Expression of Endo180 is spatially and temporally regulated during wound healing. Histopathology 2006;49:634–648. [PubMed: 17163848]

Howard MJ, Chambers MG, Mason RM, Isacke CM. Distribution of Endo180 receptor and ligand in developing articular cartilage. Osteoarthritis Cartilage 2004;12:74–82. [PubMed: 14697685]

Kjoller L, Engelholm LH, Hoyer-Hansen M, Dano K, Bugge TH, Behrendt N. uPARAP/endo180 directs lysosomal delivery and degradation of collagen IV. Exp Cell Res 2004;293:106–116. [PubMed: 14729061]

Madsen DH, Engelholm LH, Ingvarsen S, Hillig T, Wagenaar-Miller RA, Kjoller L, Gardsvoll H, Hoyer-Hansen G, Holmbeck K, Bugge TH, Behrendt N. Extracellular Collagenases and the Endocytic Receptor, Urokinase Plasminogen Activator Receptor-associated Protein/Endo180, Cooperate in Fibroblast-mediated Collagen Degradation. J Biol Chem 2007;282:27037–27045. [PubMed: 17623673]

Matziari M, Dive V, Yiotakis A. Matrix metalloproteinase 11 (MMP-11; stromelysin-3) and synthetic inhibitors. Med Res Rev 2007;27:528–552. [PubMed: 16710861]

Mousavi SA, Sato M, Sporstol M, Smedsrod B, Berg T, Kojima N, Senoo H. Uptake of denatured collagen into hepatic stellate cells: evidence for the involvement of urokinase plasminogen activator receptor-associated protein/Endo180. Biochem J 2005;387:39–46. [PubMed: 15506989]

Parks WC, Shapiro SD. Matrix metalloproteinases in lung biology. Respir Res 2001;2:10–19. [PubMed: 11686860]

Sheikh H, Yarwood H, Ashworth A, Isacke CM. Endo180, an endocytic recycling glycoprotein related to the macrophage mannose receptor is expressed on fibroblasts, endothelial cells and macrophages and functions as a lectin receptor. J Cell Sci 2000;113(Pt 6):1021–1032. [PubMed: 10683150]

Sulek J, Wagenaar-Miller RA, Shireman J, Molinolo A, Madsen DH, Engelholm LH, Behrendt N, Bugge TH. Increased expression of the collagen internalization receptor uPARAP/Endo180 in the stroma of head and neck cancer. J Histochem Cytochem 2007;55:347–353. [PubMed: 17189524]

Wu K, Yuan J, Lasky LA. Characterization of a novel member of the macrophage mannose receptor type C lectin family. J Biol Chem 1996;271:21323–21330. [PubMed: 8702911]

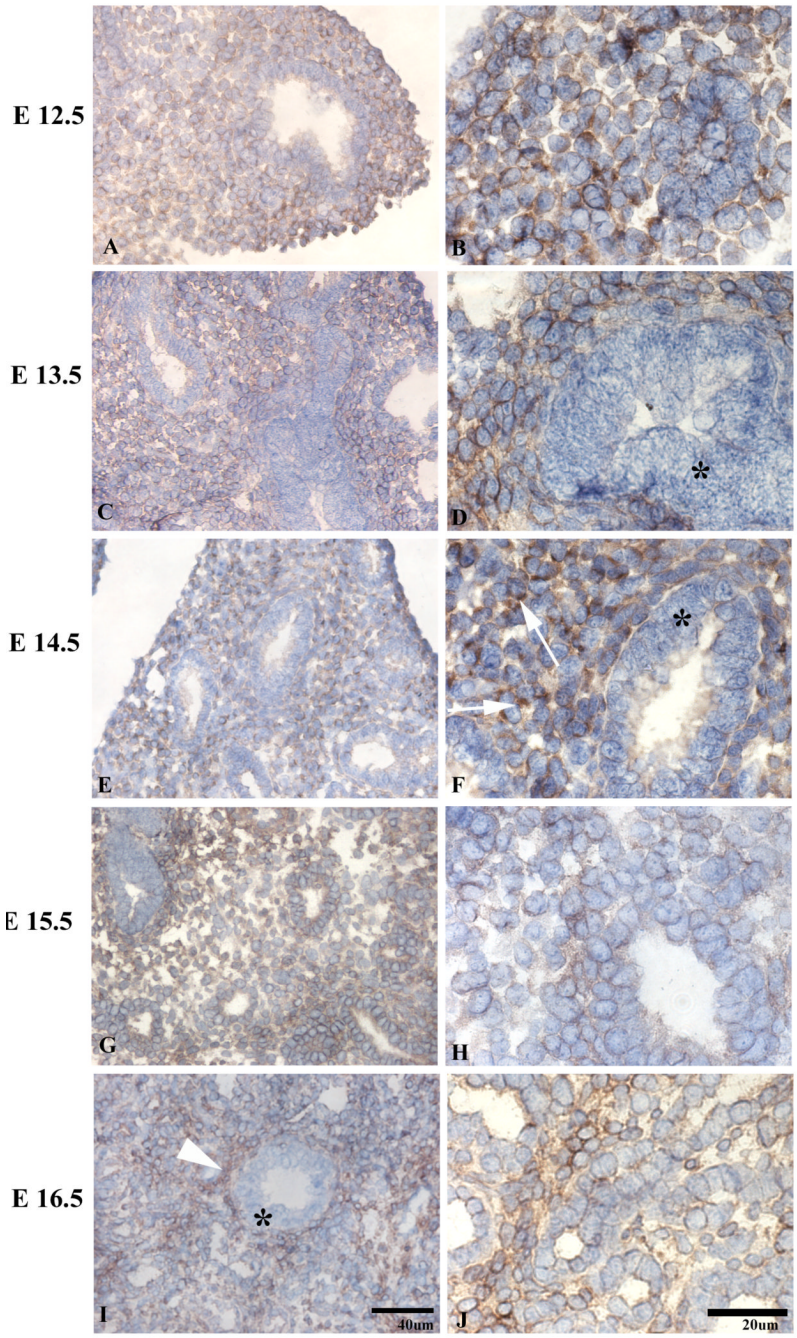

Figure 1.
Distribution of uPARAP in the pseudoglandular (A–H) and cannalicular (I–J) stages. uPARAP immunoreactivity is seen as early as E12.5 (A, B). Epithelial staining is absent (*).

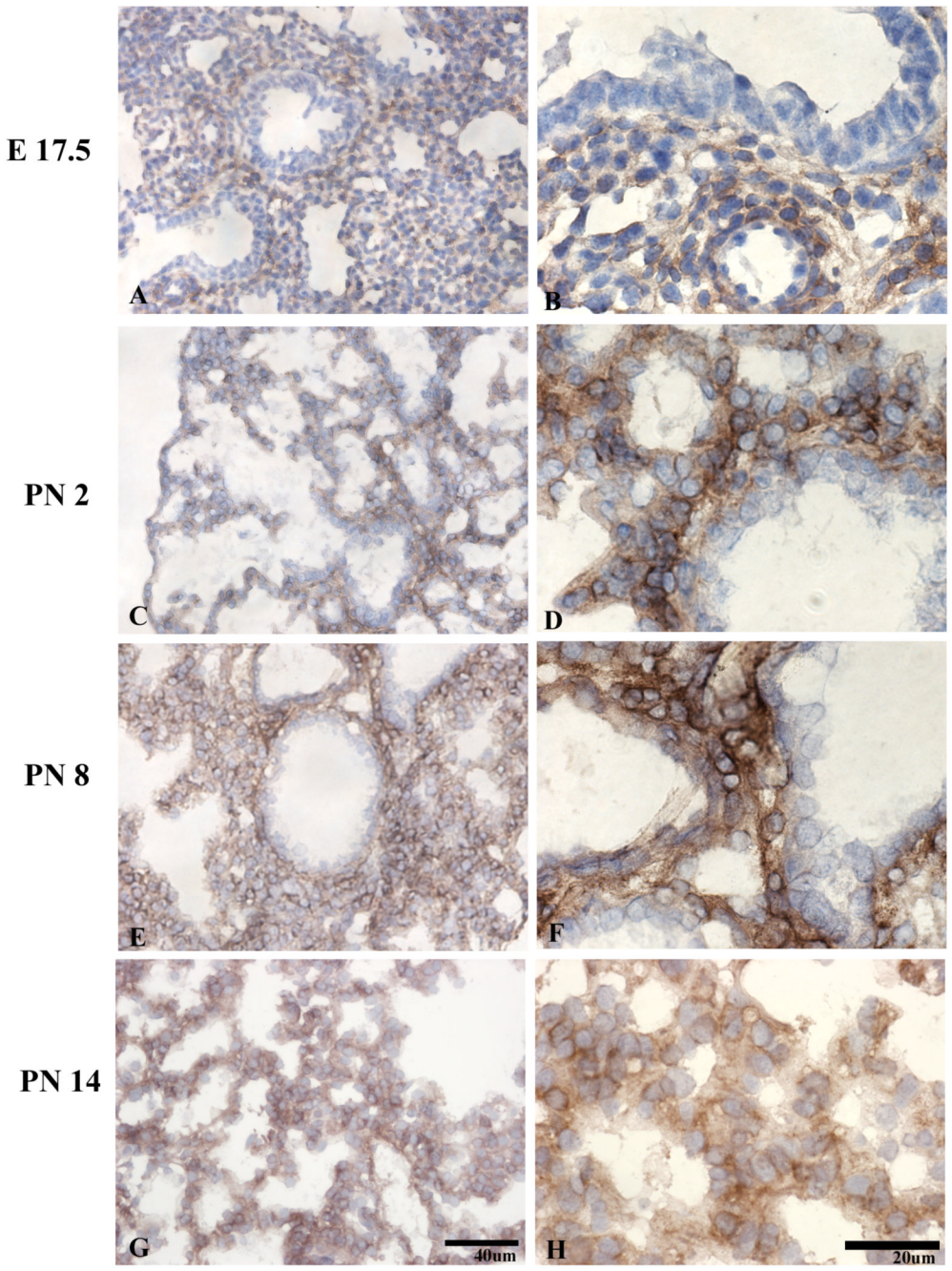

Figure 2.
Distribution of uPARAP in the late saccular (A–D) and alveolar (E–H) stages shows persistent mesenchymal uPARAP expression. The epithelium remains negative.

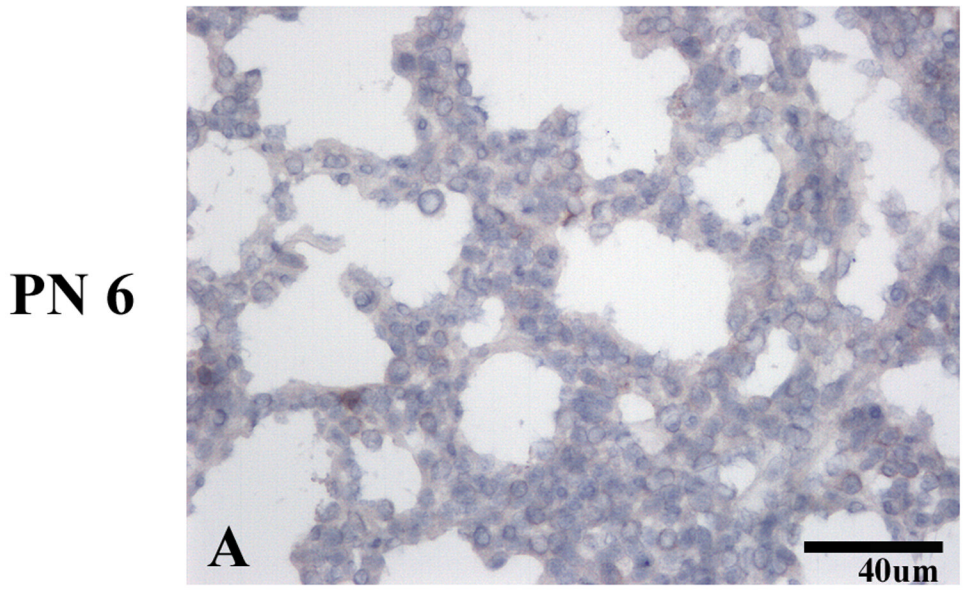

Figure 3.
Lack of uPARAP immunoreactivity on uPARAP −/− lungs.

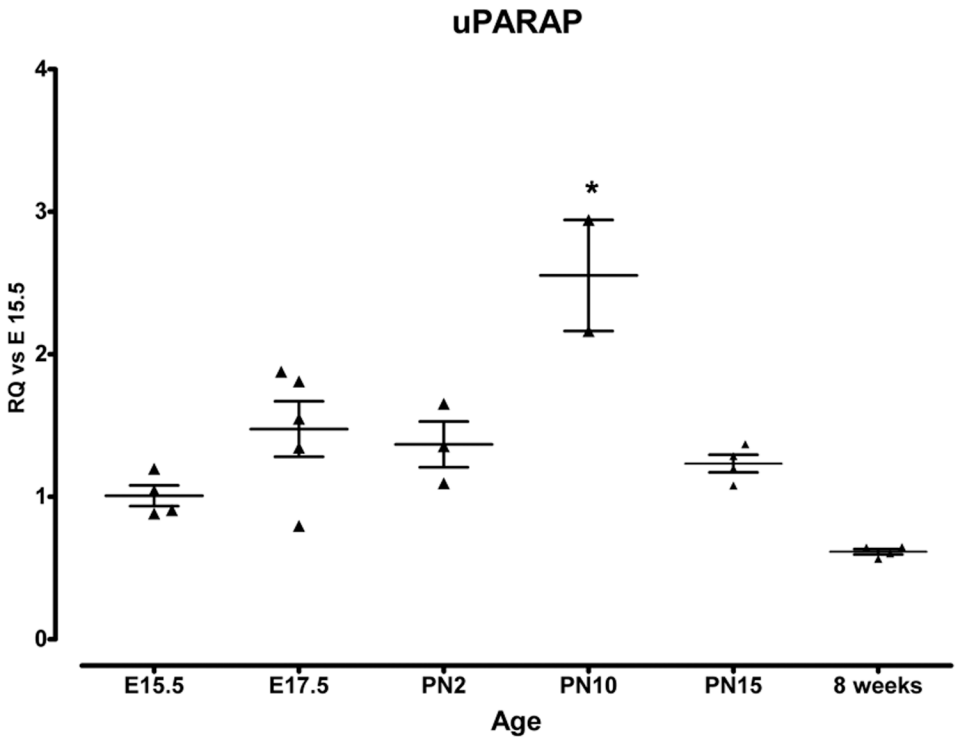

Figure 4.
Real time PCR analysis of uPARAP mRNA expression during lung development. Data were normalized to HPRT expression. Y axis represents fold increase compared to E15.5. Each point represents an individual embryo or mouse. Mean value ± SEM is indicated. * p=<0.05 compared to all other timepoints.

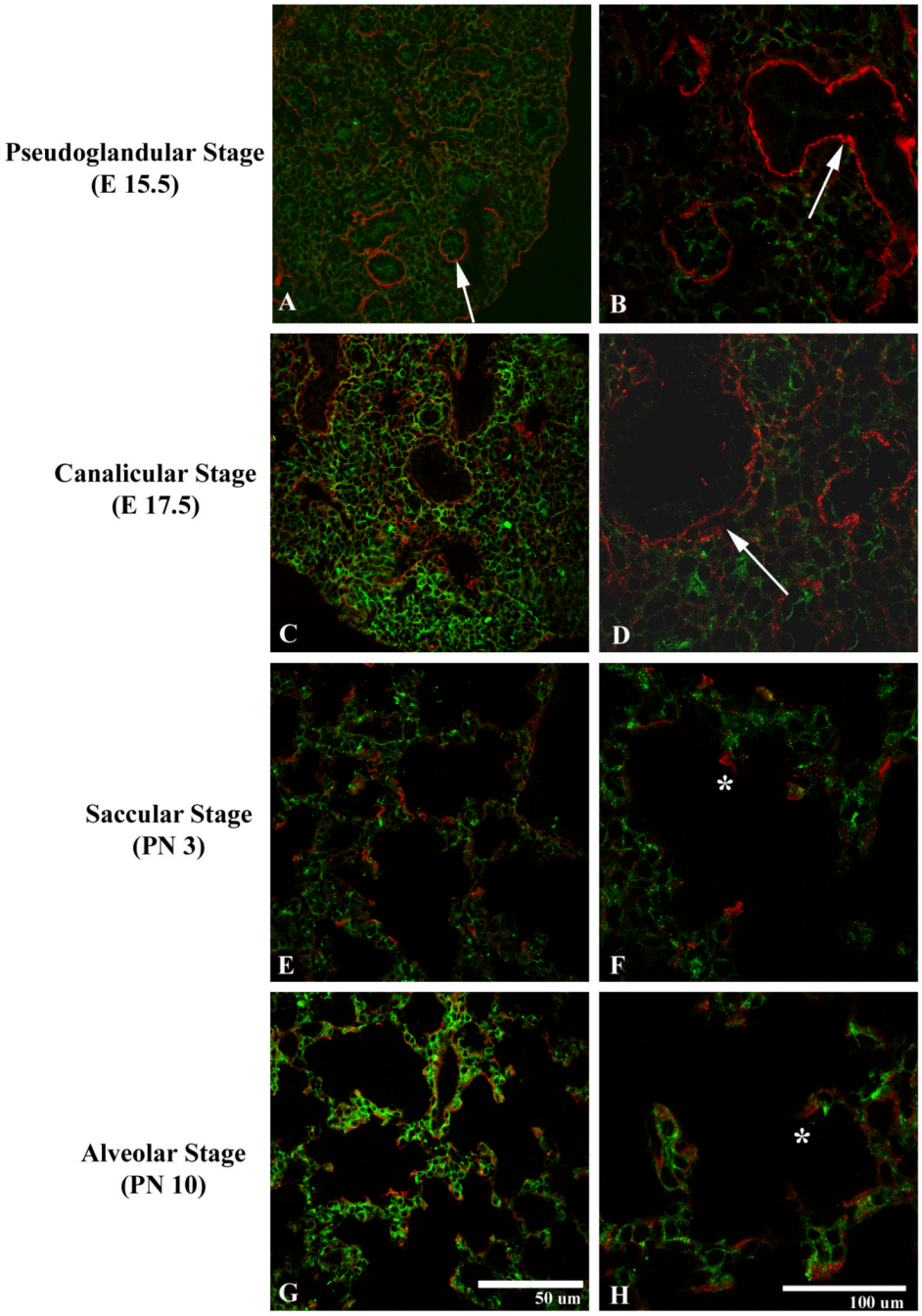

Figure 5.
Expression of uPARAP (green) and collagen I (red) during the pseudoglandular (A–B), cannalicular (C–D), saccular (E–F), and alveolar (G–H) stages. uPARAP demonstrates ubiquitous expression throughout the mesenchyme of the developing lung. Collagen I demonstrates few areas of mesenchymal staining. Collagen I is detected around developing airways (arrows) and, during later stages of development, along septal tips (*).

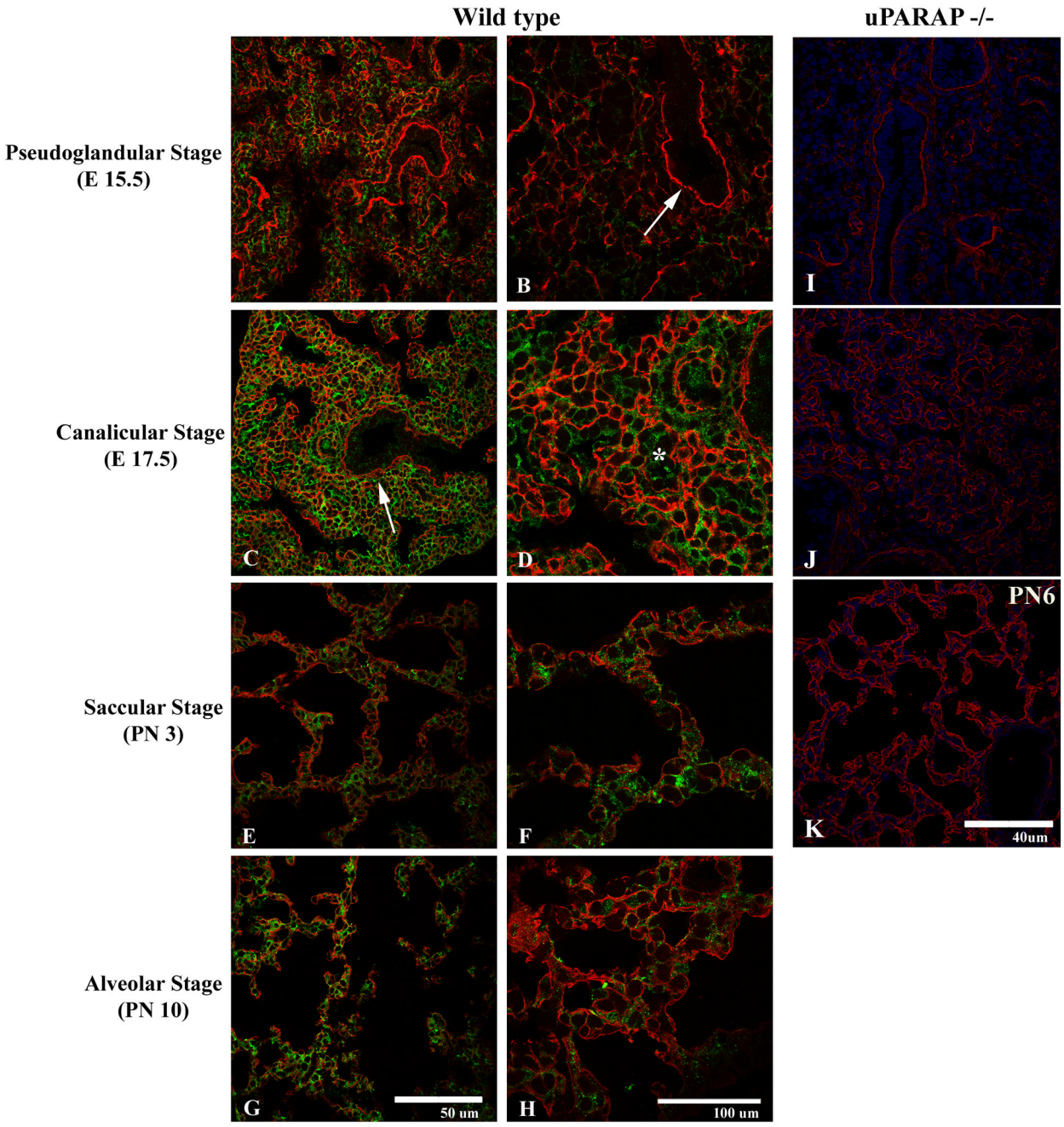

Figure 6.

Expression of uPARAP (green) and collagen IV (red) during the pseudoglandular (A–B), cannalicular (C–D), saccular (E–F), and alveolar (G–H) stages. Overlapping mesenchymal immunoreactivity for collagen IV and uPARAP is observed throughout all stages of development, particularly in the region of developing basement membranes (arrow). uPARAP expression, however, is detected in the absence of collagen IV immunoreactivity (*). I–K. Expression of collagen IV (red) in uPARAP −/− mice during pseudoglandular (I), cannalicular (J), alveolar (K) stages.

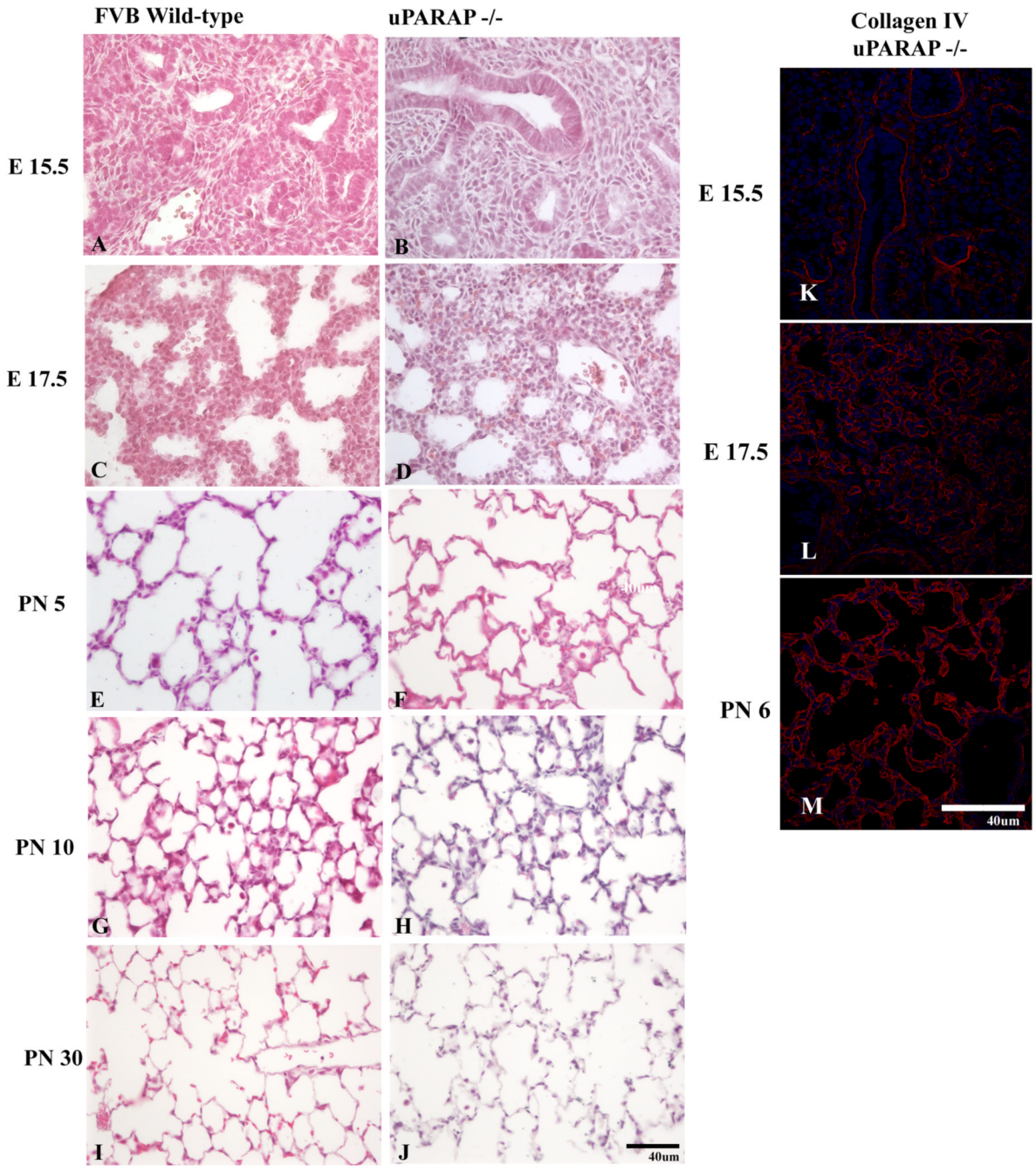

Figure 7.
Lung development in FVB wild-type and uPARAP −/− mice. Representative sections from the pseudoglandular (A, B), cannalicular (C–D), saccular (E–F), and alveolar (G–H) stages are shown for FVB wildtype and age-matched uPARAP −/− mice.

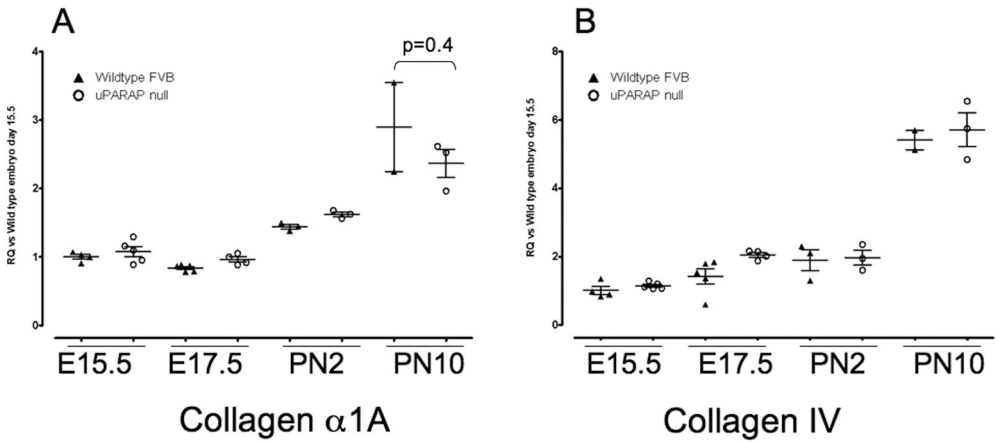

Figure 8.

Real time PCR analysis of (A) Collagen alpha1A and (B) Collagen IV mRNA expression during lung development in WT (▲) and uPARAP −/− (○) mice. Data were normalized to HPRT expression. Y axis represents fold increase compared to WT E15.5. Each point represents an individual embryo or mouse. Mean value ± SEM is indicated.

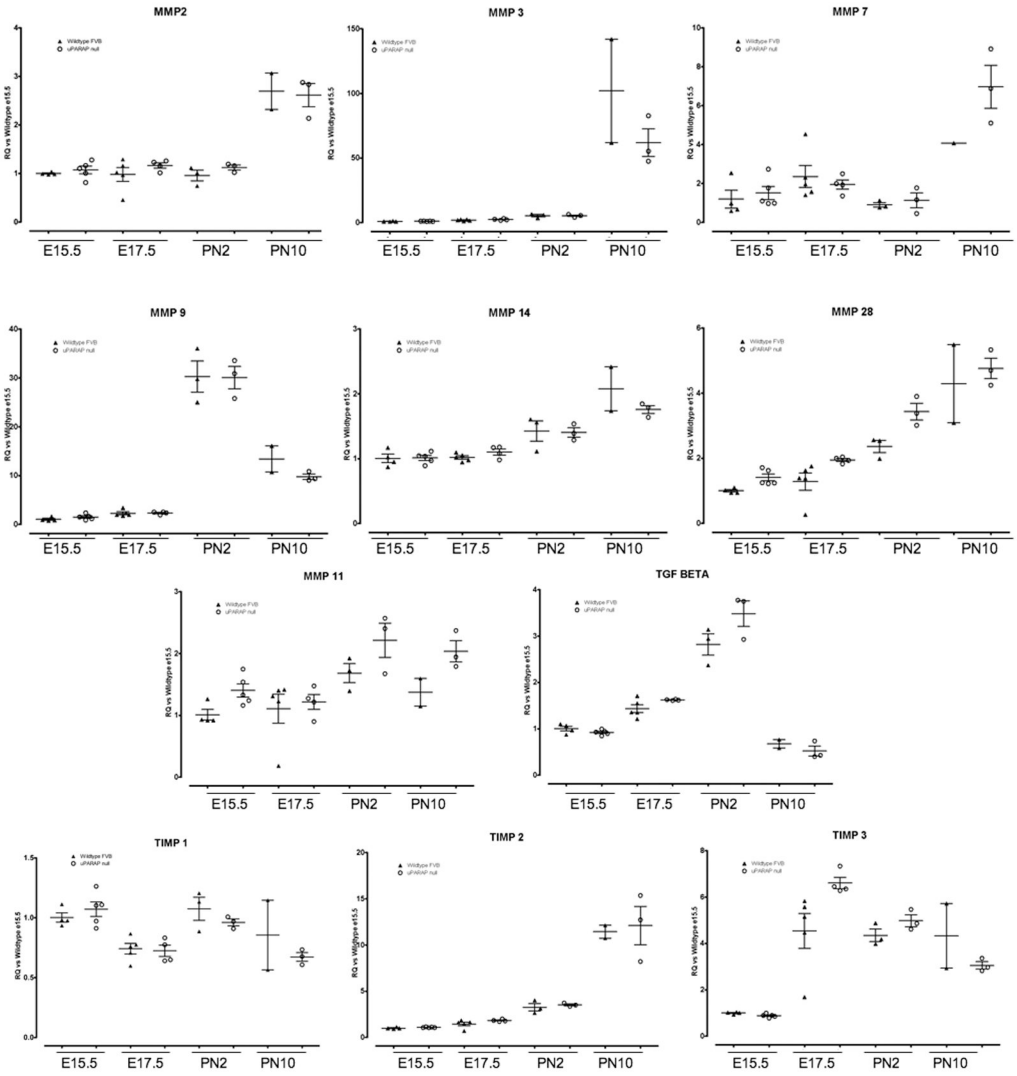

Figure 9.

Real time PCR analysis of MMPs, TIMPs and TGFβ1 expression during lung development in WT (▲) and uPARAP −/− (○) mice. Data were normalized to HPRT expression. Y axis represents fold increase compared to WT E15.5. Each point represents an individual embryo or mouse. Mean value ± SEM is indicated.